Supporting Information for

Two isostructural Zn/Co-MOFs with penetrating structures: multifunctional properties of both luminescence sensing and conversion of CO_2 into cyclic carbonates

Nana Liu[a,b#], Tingting Liu[a#], Guangning Liu[b], Xiuna Mi[a], Yunwu Li[a], Lu Yang[c], Zhen Zhou[c], Suna Wang[a,b]*

[a] Shandong Provincial Key Laboratory of Chemical Energy Storage and Novel Cell Technology, School of Chemistry and Chemical Engineering, Liaocheng University, Liaocheng, 252059, P. R. China

[b] School of Chemistry and Chemical Engineering, University of Jinan, Jinan, Shandong, 250022, P. R. China

[c] School of Chemistry and Chemical Engineering, Shandong University of Technology, Zibo, 255000, P. R. China

Email: wangsuna@lcu.edu.cn; zhouzhen@sdut.edu.cn

# These two authors contribute equally.

Table of Content

Fig. S13 (a) and (b) CO_2 adsorption isotherms for **Zn-MOF-1** and **Co-MOF-2** with fitting by Virial 2 model.

Fig. S14 (a) and (b) The PXRD of **Zn-MOF-1** and **Co-MOF-2** before and after the cyclic experiment.

Fig. S15 (a) and (b) FT-IR of **Zn-MOF-1** and **Co-MOF-2** after cyclic experiment.

X-ray crystallographic study

Single-crystal X-ray data for **Zn-MOF-1** and **Co-MOF-2** were collected on a Siemens Smart CCD diffractometer with graphite-monochromatic Mo Kα radiation (λ = 0.71073 Å) at 298 K. The raw data frames were integrated into SHELX-format reflection files and corrected using SAINT program. Absorption corrections based on multi-scan were obtained by the SADABS program. The structure was solved with direct methods (SHELXS) and refined with full-matrix least-squares technique using the SHELXL-2014/7 programs. Displacement parameters were refined anisotropically, and the positions of the H-atoms were generated geometrically, assigned isotropic thermal parameters, and allowed to ride on their parent carbon atoms before the final cycle of refinement. PLATON/SQUEEZE was employed to calculate the contribution to the diffraction in the channels and produced a set of solvent-free diffraction intensities. The final formula was calculated from the SQUEEZE (A. L. Spek, J. Appl. Crystallogr. 2003, 36, 7) results combined with elemental analysis data and TGA data.Basic information pertaining to crystal parameters and structure refinement is summarized in Table S1. Selected bond lengths and angles are listed in Table S2.

Table S1. Refined crystal parameters of **Zn-MOF-1** and **Co-MOF-2**.

Compound	**Zn-MOF-1**	**Co-MOF-2**
CCDC	2301443	2301442
Formula	$C_{31}H_{29}ZnN_3O_8$	$C_{31}H_{29}CoN_3O_8$
Formula weight	637.19	630.71
T [K]	298.15(2)	298.15(2)
Crystal system	Orthorhombic	Orthorhombic
Space group	$P2_12_12$	$P2_12_12$
a [Å]	13.6458(13)	13.6420(12)
b [Å]	21.7476(19)	21.8159(17)
c [Å]	10.1293(9)	10.0776(9)
α [°]	90	90
β [°]	90	90
γ [°]	90	90
V [Å^3]	3006.0(5)	2999.2(4)
Z	4	4
$D_{calcd.}$ [g·cm^{-3}]	1.407	1.396
μ [mm^{-1}]	0.872	0.627
θ range	2.40-25.02	2.39-25.02
index ranges	$-16 \leq h \leq 8$ $-25 \leq k \leq 25$ $-11 \leq l \leq 12$	$-16 \leq h \leq 15$ $-20 \leq k \leq 25$ $-10 \leq l \leq 11$
R1; wR_{2a} [I > 2σ(I)]	0.0367; 0.0624	0.0324; 0.0633
GOF	0.981	1.054

$^aR_1 = \Sigma| |F_o|-|F_c| |/ \Sigma|F_o|$, $^bwR_2 = [\Sigma w(F_o^2-F_c^2)^2]/ \Sigma w(F_o^2)^2]^{1/2}$

Table S2. Selected bond lengths [Å] and angles [º] for **Zn-MOF-1** and **Co-MOF-2**.

Zn-MOF-1			
Zn(1)-O(4)	1.973(3)	Zn(1)-O(6)	1.988(3)
Zn(1)-N(1)	2.051(3)	Zn(1)-N(2)	2.037(3)
O(4)-Zn(1)-O(6)	98.30(11)	O(4)-Zn(1)-N(1)	111.50(15)
O(4)-Zn(1)-N(2)	112.42(15)	N(2)-Zn(1)-N(1)	111.69(14)
O(6)-Zn(1)-N(1)	114.71(14)	O(6)-Zn(1)-N(2)	107.53(14)
Co-MOF-2			
Co(1)-O(4)	1.988(3)	Co(1)-O(6)	1.985(3)
Co(1)-N(1)	2.046(3)	Co(1)-N(2)	2.060(4)
O(4)-Co(1)-O(6)	96.02(12)	O(4)-Co(1)-N(1)	107.88(15)
O(4)-Co(1)-N(2)	115.58(15)	N(2)-Co(1)-N(1)	111.70(15)
O(6)-Co(1)-N(1)	112.01(15)	O(6)-Co(1)-N(2)	112.69(15)

Table S3. Time tracing of **Zn-MOF-1** catalyzed CO_2 cycloaddition of epoxide.

Entry	**Substrate (**10mmol**)**	**Catalyst**	**Co-Cat.** TBAB	**T** °C	**P** MPa	**t** h	**Yield** %
1	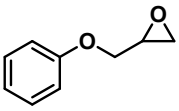	**1**\4mg	64.4mg	70	0.5	3	22
2	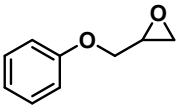	**1**\4mg	64.4mg	70	0.5	6	57
3	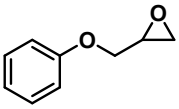	**1**\4mg	64.4mg	70	0.5	9	88
4	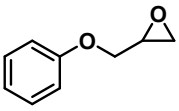	**1**\4mg	64.4mg	70	0.5	12	96
5	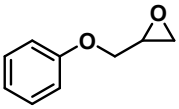	**1**\4mg	64.4mg	70	0.5	14	98

Table S4. Pressure tracing of **Zn-MOF-1** catalyzed CO_2 cycloaddition of epoxide.

Entry	**Substrate**	**Catalyst**	**Co-Cat.**	**T**	**P**	**t**	**Yield**

	10mmol		TBAB	℃	MPa	h	%
1	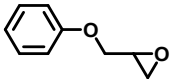	**1**\4mg	64.4mg	70	0.1	12	15
2	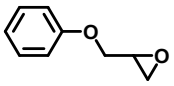	**1**\4mg	64.4mg	70	0.3	12	61
3	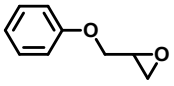	**1**\4mg	64.4mg	70	0.5	12	96
4	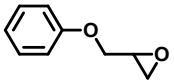	**1**\4mg	64.4mg	70	0.7	12	97
5	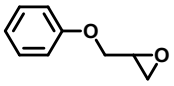	**1**\4mg	64.4mg	70	1	12	99

Table S5. CO_2 cycloaddition of different epoxides catalyzed by **Zn-MOF-1** and **Co-MOF-2**.

Entry	**Substrate** 10mmol	**Catalyst**	**Co-Cat.** TBAB	**T** °C	**P** MPa	**t** h	**Yield%** **1**	**2**
1	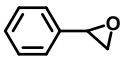	**1**\4mg **2**\4mg	64.4mg	70	0.5	12	65	53
2	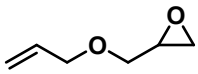	**1**\4mg **2**\4mg	64.4mg	70	0.5	12	87	77
3	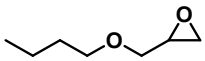	**1**\4mg **2**\4mg	64.4mg	70	0.5	12	80	72
4	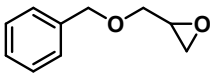	**1**\4mg **2**\4mg	64.4mg	70	0.5	12	83	79
5	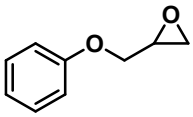	**1**\4mg **2**\4mg	64.4mg	70	0.5	12	96	92

Table S6. Investigation of some substrates in the CO_2-to-epoxide cycloaddition reaction (substrate in entry 4 and 5 in Table 1) catalyzed by $Zn(NO_3)_2{\cdot}6H_2O$ and

$Co(NO_3)_2 \cdot 6H_2O$ in the presence of TBAB as the cocatalyst.

Entry	catalyst	Substrate	Product	Yield%
1	$Zn(NO_3)_2 \cdot 6H_2O$	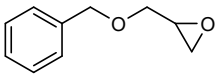	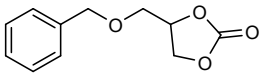	65
2	$Zn(NO_3)_2 \cdot 6H_2O$	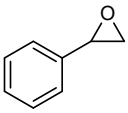	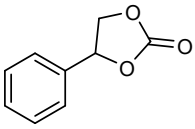	79
3	$Co(NO_3)_2 \cdot 6H_2O$	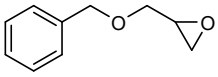	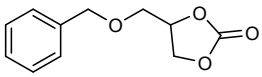	47
4	$Co(NO_3)_2 \cdot 6H_2O$	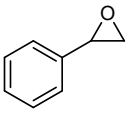	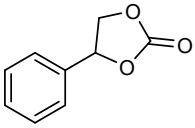	73

Reaction conditions: epoxide (10 mmol), catalyst (0.1 mol %), and TBAB (0.2 mmol) under CO_2 (0.5 MPa), 70 ^{o}C, 12 h.

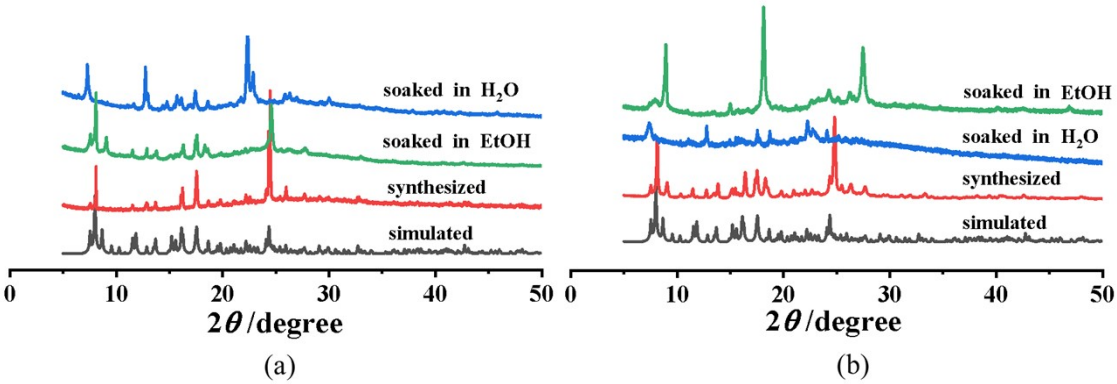

Fig. S1 (a) and (b) PXRD spectra of **Zn-MOF-1** and **Co-MOF-2** soaked in EtOH and H_2O**.**

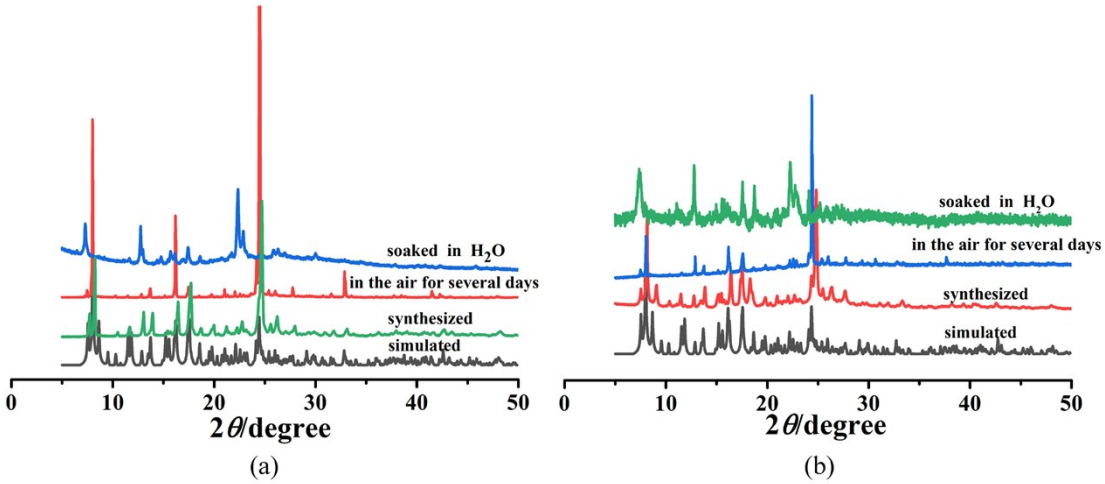

Fig. S2 (a) and (b) PXRD spectra of **Zn-MOF-1** and **Co-MOF-2**: Newly-synthesized samples, exposed in air for five days, immersed in water for three days.

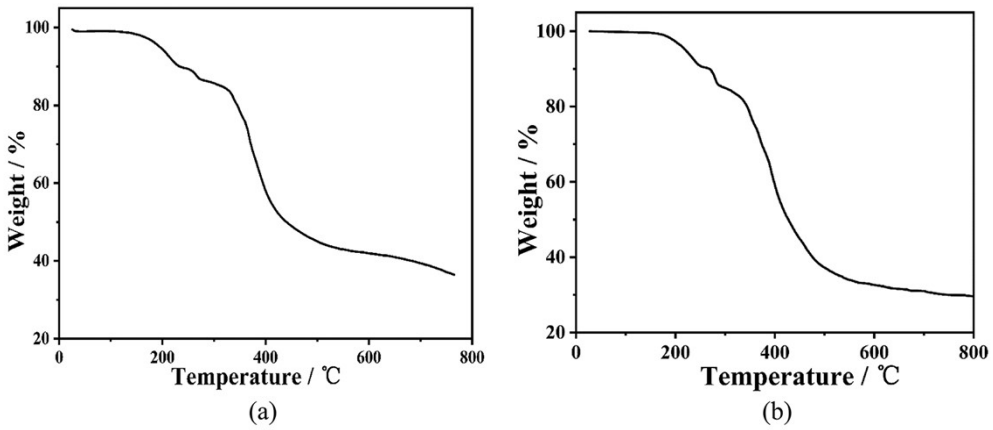

Fig. S3. (a) and (b) TG of **Zn-MOF-1** and **Co-MOF-2**, respectively.

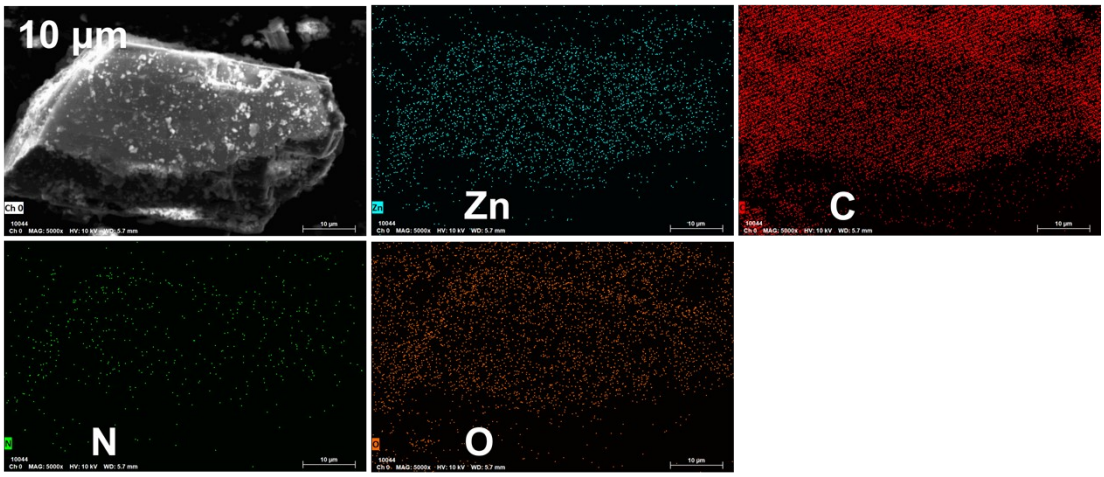

(a)

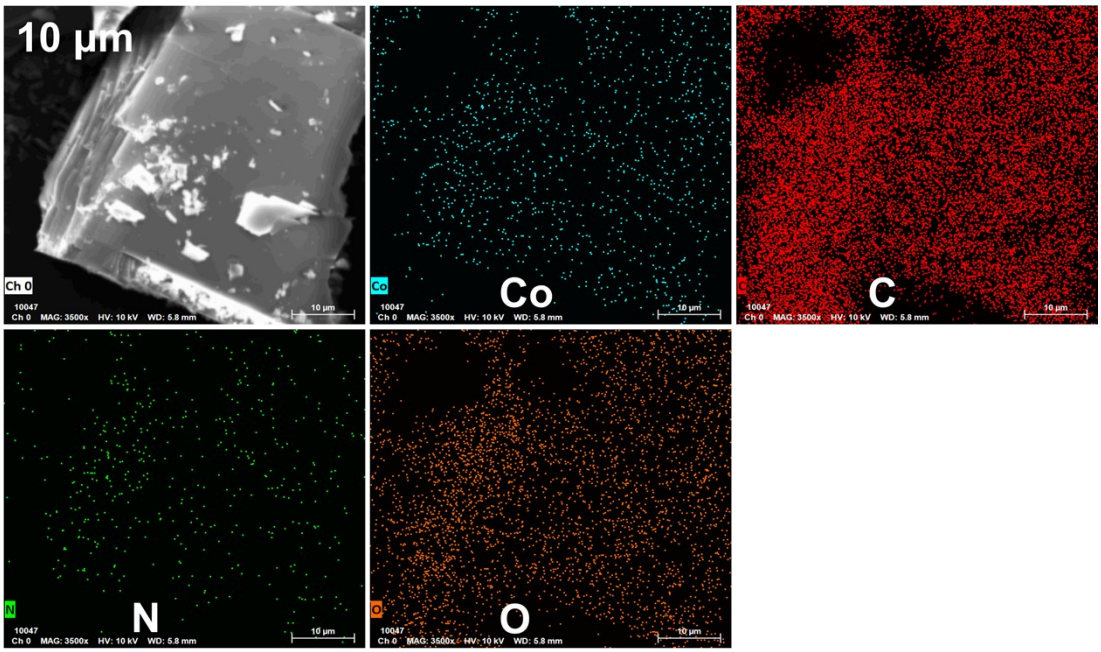

(b)

Fig. S4 (a) and (b) EDS mapping of **Zn-MOF-1** and **Co-MOF-2**.

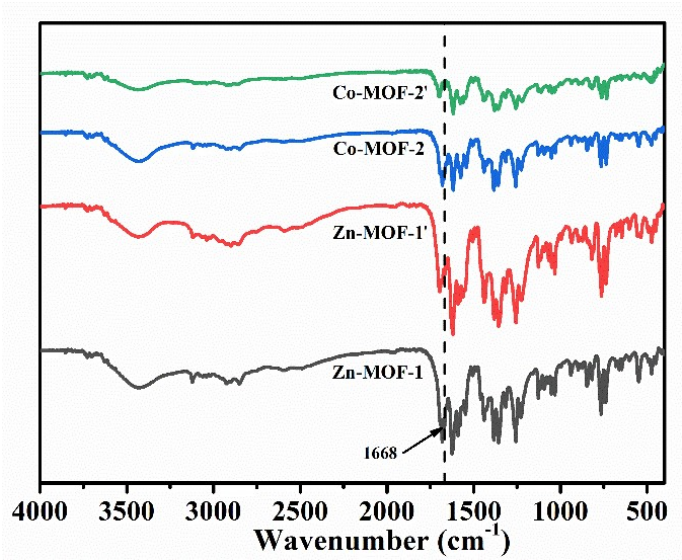

Fig. S5 (a) and (b) IR of **Zn-MOF-1** and **Co-MOF-2** before and after activation, respectively.

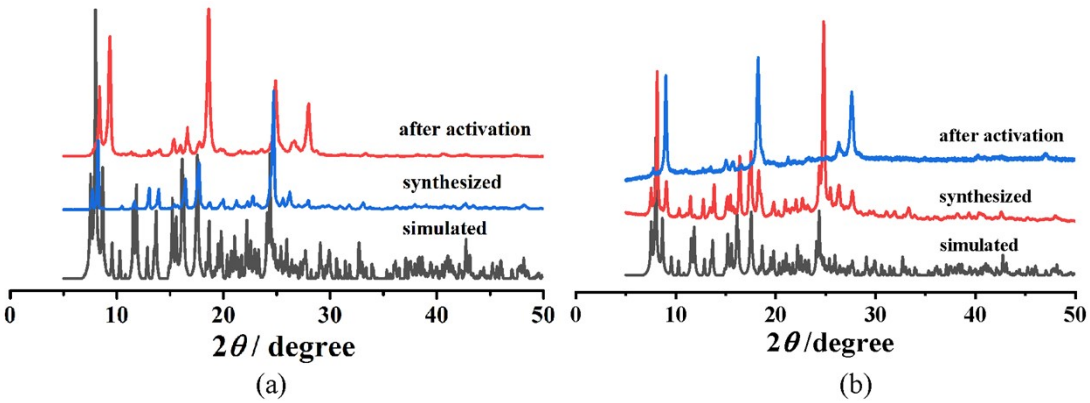

Fig. S6 (a) and (b) PXRD spectra of **Zn-MOF-1** and **Co-MOF-2** before and after activation, respectively.

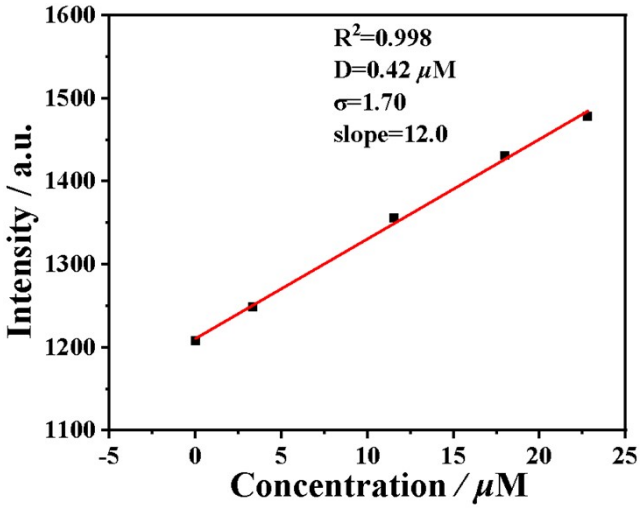

Fig. S7 Calculation of detection limit of **Zn-MOF-1** toward Al^{3+}.

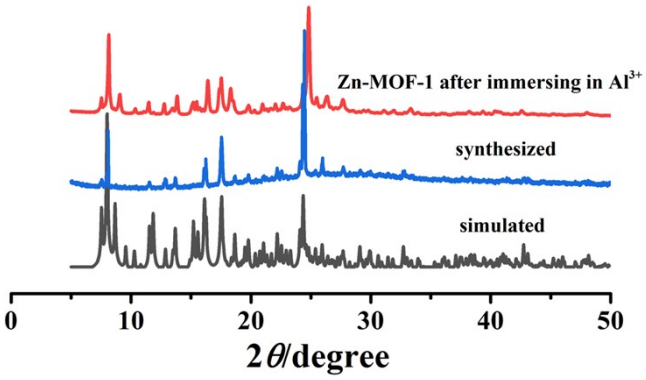

Fig. S8 PXRD spectra of **Zn-MOF-1** after soaking in EtOH solution of Al^{3+} for three days.

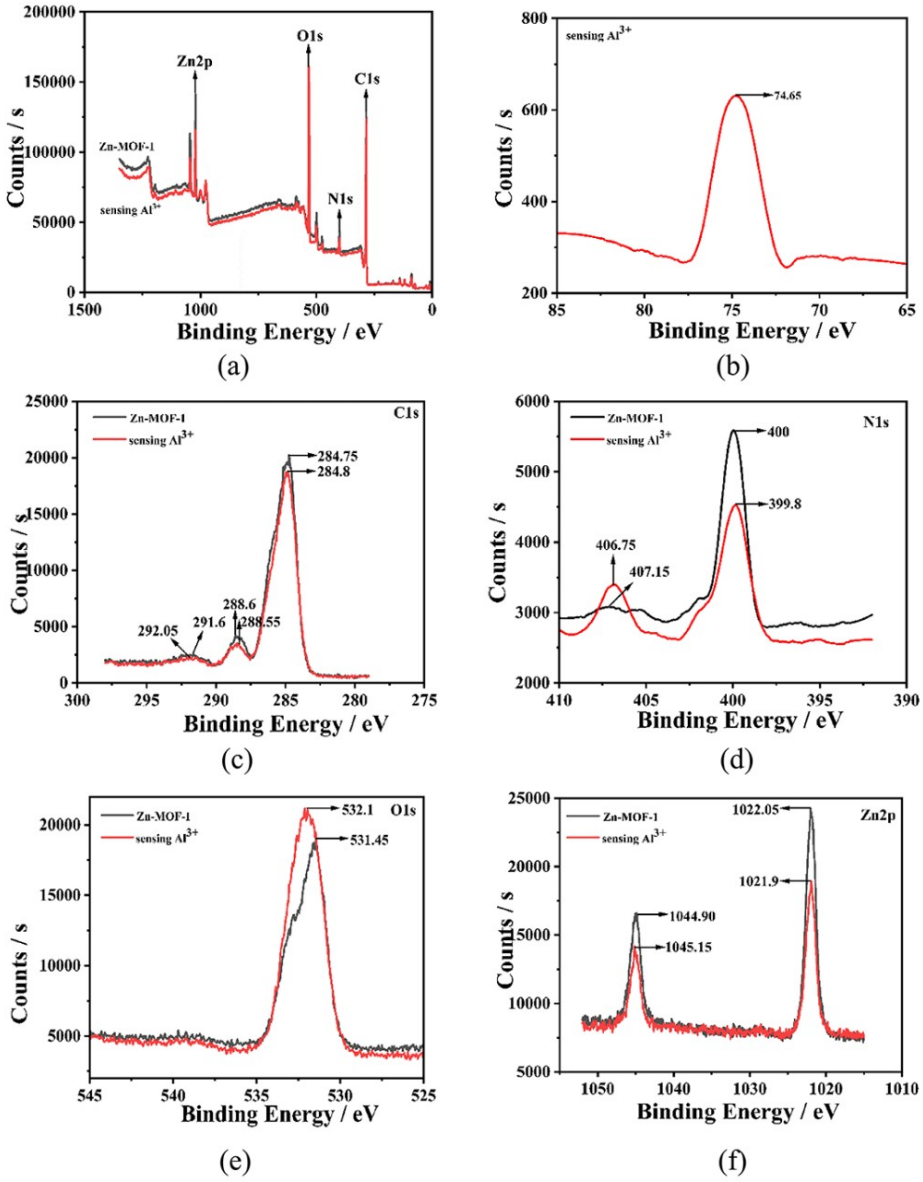

Fig. S9 XPS spectra of **Zn-MOF-1** before and after treatment in EtOH solution of Al^{3+}.

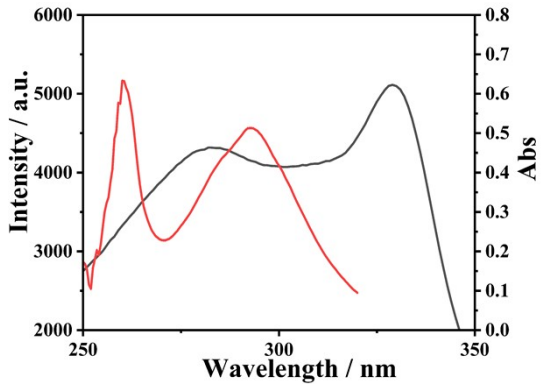

Fig. S10 UV−vis spectra of **Zn-MOF-1** soaked in EtOH solution of Al^{3+} ions (10^{-3} M).

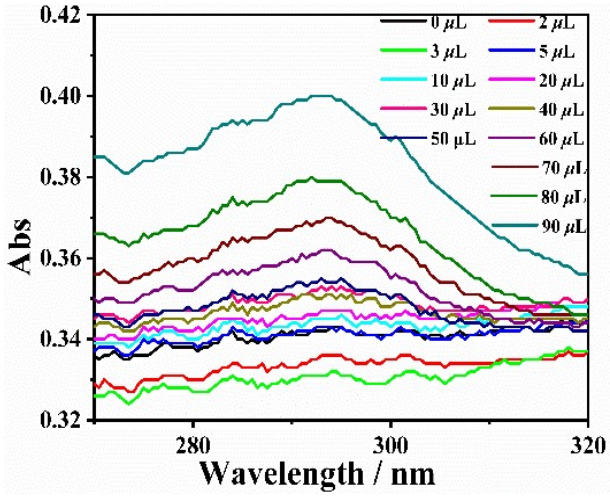

Fig. S11 UV−vis spectra of **Zn-MOF-1** soaked in different concentration of Al^{3+} ions (10^{-3} M).

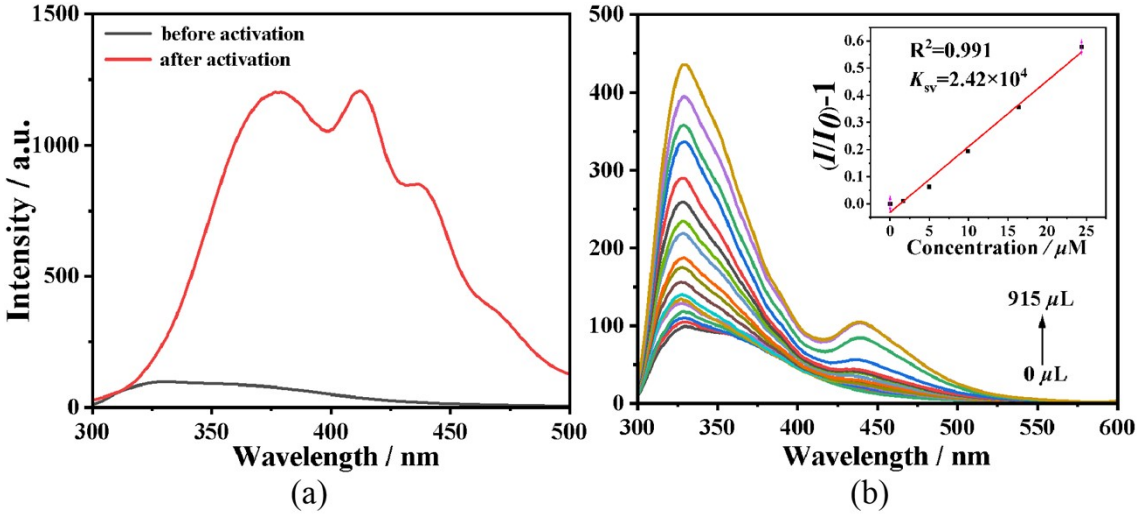

Fig. S12 (a) The fluorescence spectra of **Zn-MOF-1** before and after activation. (b) The fluorescence titration result of the activated **Zn-MOF-1'** toward Al^{3+}. Insert: S-V plot.

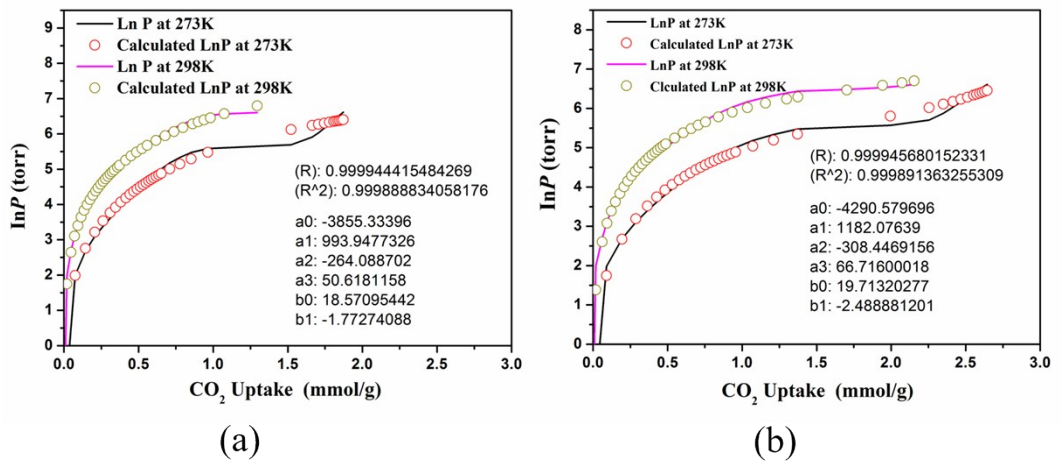

(a) (b)

Fig. S13 (a) and (b) CO_2 adsorption isotherms for **Zn-MOF-1** and **Co-MOF-2** with fitting by Virial 2 model.

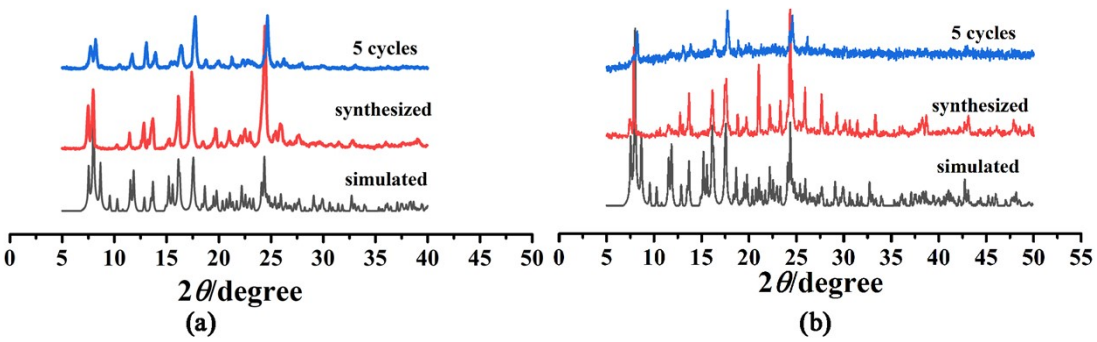

Fig. S14 (a) and (b) The PXRD of **Zn-MOF-1** and **Co-MOF-2** before and after the cyclic experiment.

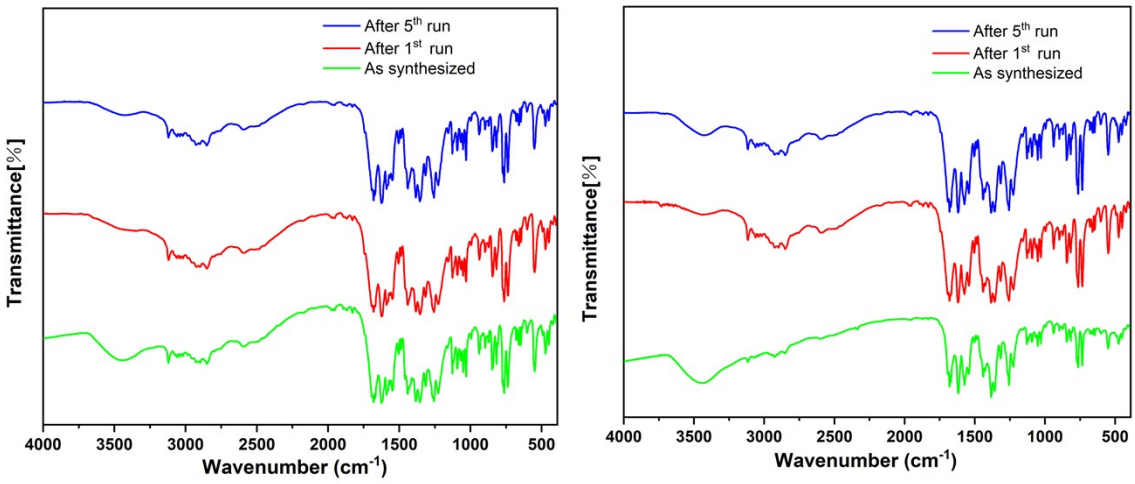

(a) (b)

Fig. S15 (a) and (b) FT-IR of **Zn-MOF-1** and **Co-MOF-2** after cyclic experiment.